

## Asymmetric Ground Structured Circularly Polarized Antenna for ISM and WLAN Band Applications

Badugu P. Nadh, Boddapati T. P. Madhav\*, Munuswamy S. Kumar, Manikonda V. Rao, and Tirunagari Anilkumar

**Abstract**—This article presents the design and analysis of a dual-band antenna with circular polarization for ISM and WLAN band applications. The proposed antenna operates at two frequencies ranging from 2.1–3.1 GHz and 4.4–7.7 GHz with resonating frequencies at 2.45 GHz industrial, scientific and medical band (ISM) and 5.8 GHz wireless local area network band (WLAN). The antenna is fed by coplanar waveguide feeding (CPW) with an asymmetric ground structure, and the radiating element consists of 24 spokes in the design. The current antenna providing the impedance bandwidths of 38.4% and 49% at two operating bands. The proposed antenna exhibiting circular polarisation with 3 dB axial ratio bandwidth of 150 MHz at 2.33–2.48 GHz and 1600 MHz at 5.14–6.74 GHz. The designed antenna is fabricated on an RT Duroid 5880 substrate with dimensions of  $40 \times 28 \times 0.4 \text{ mm}^3$ . The intension behind the design of this antenna is to use it for wearable applications in conformal nature with low specific absorption rate (SAR). The SAR values observed at two operating frequencies are 1.09 W/Kg and 1.47 W/Kg on hand and 0.946 W/Kg and 1.12 W/Kg on head, respectively. The placement and radiation characteristics analysis is done with Ansys Savant tool, and the subsequent measured results provide good correlation with simulation results.

### 1. INTRODUCTION

ISM band based wearable antennas are getting their significance in medical industry to improve the quality of communication service [1]. These antennas are used in many applications like telemedicine, military, sports and in emerging new technologies [2]. To cover these applications, designed antennas need to cover WBAN frequencies like 2.4 GHz (2.4–2.485) GHz and 5.8 GHz (5.725–5.875) GHz [3]. Owing to significant demand for these frequency bands, several efforts have been made to design dual-band antennas with compact size, flexibility and good operating characteristics [4]. To place the antenna on human body there are some limitations to be considered such as size, safety and low propagation losses inside the conductive layers [5]. The antenna is placed on high dielectric constant layers like skin which leads to frequency disturbance and back radiation influence by the human layers and causes biological effects.

In the literature, various antennas have been designed to achieve good on-body communication [6]. A monopole antenna is designed with inverted L-shape for ISM applications covering (2.42–2.48 GHz) and (5–6 GHz) [7]. The multiband antenna is designed to cover three ISM bands at 2.4–2.48 GHz, 5.15–5.35 GHz and 5.7–5.8 GHz [8]. A dual-band monopole patch antenna is designed with CPW feeding for on/off-body communication operating at medical (ISM) bands covering 2.45 GHz and 5.8 GHz respectively. A fan-shaped antenna is designed with shorting stubs and crumpling nature in [9]. A shorted patch antenna of parasitic elements with omnidirectional patterns at 2.45 GHz and 5.8 GHz

---

*Received 14 September 2018, Accepted 21 November 2018, Scheduled 11 December 2018*

\* Corresponding author: Boddapati T. P. Madhav (btpmadhav@kluniversity.in).

The authors are with the Antennas and Liquid Crystals Research Center, Department of Electronics and Communication Engineering, Koneru Lakshmaiah Education Foundation, AP, India.

is presented in [10]. A circular monopole patch antenna with four symmetric slots is designed for omnidirectional radiation pattern and operating in ISM band. A circularly polarised antenna with asymmetric crossed bowtie dipoles is designed to cover medical band frequencies with axial ratio bandwidths of 57% and 51% [11]. A circularly polarised antenna is designed with a Taconic RF-35 substrate which covers the GPS, WiMAX, WLAN, and radio altimeter applications [12]. A foldable thin circular monopole antenna is designed with liquid crystalline polymer substrate for wearable applications with different bending conditions [13]. A tai-chi-shaped antenna is designed with circular polarisation for dual-band applications in [14]. A conformal antenna is designed on a paper substrate with graphene as a radiating element instead of copper in [15]. Shin et al. [17] proposed a meander line monopole antenna for PCS/IMT-2000/WLAN handsets with reduction in the SAR value. Ahmed et al. [18] presented an eagle-shaped wearable MIMO antenna with reduction of mutual coupling to 36 dB by placing EBG structure between antenna elements.

In this article, a circular ring-shaped antenna with 24 spokes is designed to attain dual-band frequency. The designed antenna is fed by CPW feeding, and a novel asymmetric ground structure is taken in this model. Dual operating bands for ISM and WLAN applications are aimed in this article with circular polarisation. To test the antenna for wearable applications, different bending effects at different bending angles are analyzed and presented in this work. A novel compact structured antenna of dual-band operation at medical communication bands with circular polarization is an attractive feature of this model. The designed model provides excellent impedance characteristics and peak realized gain of 4.6 dBic.

## 2. ANTENNA DESIGN AND DIMENSIONS

The topology of the antenna is presented in Fig. 1. The prototyped antenna is designed on a semi-flexible substrate of Rogers Duroid 5880 material with dielectric constant of 2.2 and loss tangent of 0.007. The overall dimension of the antenna is  $40 \times 28 \times 0.4 \text{ mm}^3$ . The constructed antenna consists of a circular ring with CPW feeding as shown in iteration 1. In iteration 2, 8 spokes are added to the circular ring and are separated by an angle of  $45^\circ$  each, with each spoke connected to the ring. In iterations 3, eight spokes are replaced with 16 spokes, which are separated by an angle of  $22.5^\circ$ . In the proposed model, 16 spokes are replaced with 24 spokes, and each spoke is separated by an angle of  $15^\circ$ . In between the spokes, a circle with radius of 0.6 mm is taken to separate the spokes on the circular ring. At the center of radiating patch, a circular slot is made with radius of 1 mm. In the ground

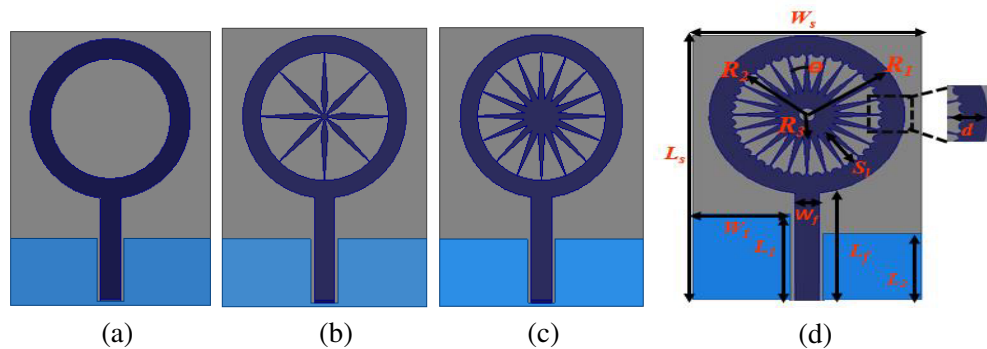


**Figure 1.** (a) Circular antenna. (b) Ring antenna with 8 spokes. (c) Ring antenna with 16 spokes. (d) Proposed antenna dimensions with 24 spokes.

**Table 1.** Parameters of circular ring antenna.

Parameter	$L_s$	$W_s$	$L_f$	$W_f$	$W_1$	$L_1$	$L_2$	$S_l$	$R_1$	$R_2$	$R_3$	$\theta$	$d$
Value (mm)	40	28	16	3	12	13	10	5.5	12	9.5	3.5	15	2.5

plane, an asymmetric structure is taken with lengths of ‘ $L_1$ ’ and ‘ $L_2$ ’ to attain circular polarisation. Table 1 presents dimensions of the proposed antenna in mm. The circular ring structure is derived from a circular patch whose radius ‘ $R_1$ ’ is calculated using the given formula [13].

$$R_1 = \frac{F}{\left\{ 1 + \frac{2h}{\pi\epsilon_r} \left[ \ln \left( \frac{\pi F}{2h} \right) + 1.7726 \right] \right\}^{1/2}} \tag{1}$$

### 3. RESULTS AND DISCUSSIONS

The basic circular ring antenna producing resonating frequency at 2.1 GHz with frequency ranging from 1.8 to 2.7 GHz, which covers GSM-1.8/1.9 GHz, Digital communication band (1.8 GHz), UMTS (1.9 GHz) and Industrial scientific medical bands (2.45 GHz) and lower band WLAN applications. When eight spokes and sixteen spokes are added to the circular ring structure, the antenna resonates at 2.45 GHz ranging from 2 to 2.8 GHz.

When 24 spokes are loaded to the antenna structure, it operates in the dual bands at resonating frequencies of 2.45 GHz and 5.8 GHz, respectively. The first frequency band ranging from 2.1 to 3.1 GHz with bandwidth of 1 GHz covering ISM band and second band ranging from 4.4 to 7.3 GHz with bandwidth 2.9 GHz covering WLAN applications band. In Fig. 2(b) the peak gain of the antenna and axial ratio are presented. The antenna shows maximum peak gain of 2.2 dBic at 2.45 GHz and 4.6 dBic at 5.8 GHz. The antenna provides circular polarisation with 3 dB axial ratio of 150 MHz and 1600 MHz at two resonating frequencies.

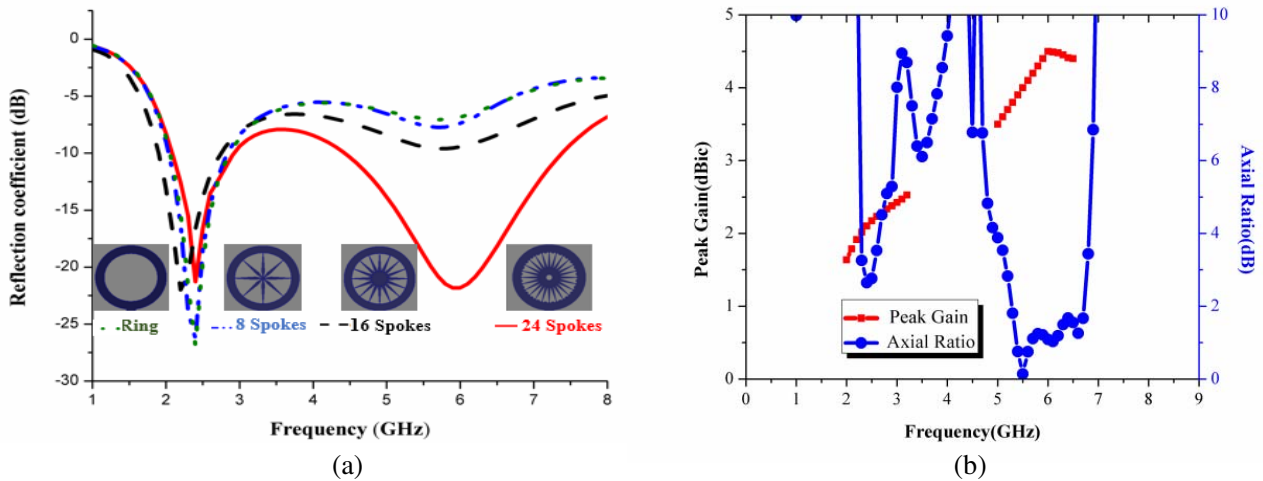


**Figure 2.** Antenna performance characteristics. (a) Reflection coefficients of the antenna iterations. (b) Peak gain and axial ratio of the proposed antenna.

A parametric study is carried out to analyze critical parameters that will tune the antenna functionality. The parametric studies of reflection coefficient for different values of  $R_2$ ,  $R_3$ ,  $L_1$  and  $W_f$  are presented in Fig. 3. In this analysis, one parameter is varied, and all other parameters are kept constant. The inner circle radius is varied from 8.5 to 10 mm with step size of 0.5 mm and presented in Fig. 3(a). For the lower values of  $R_2$ , the antenna shows single frequency band at 2.45 GHz. When the value of  $R_2$  is varied from 8.5 to 9.5 mm, antenna resonates at dual bands of 2.45 GHz and 5.8 GHz, respectively. Similarly, when circle radius  $R_3$  is varied from 2.5 to 4.5 mm, antenna operates in the dual bands for  $R_3 = 3.5$  mm, and for other values it does not show any resonating frequency at 5.8 GHz.

Similarly the length of the ground ( $L_1$ ) is varied from 11 to 14 mm, and as the length of ground increases, there is a variation in the second resonant band at 5.8 GHz. The designed antenna shows circular polarization with an asymmetric ground structure. So, the ground structure is studied by

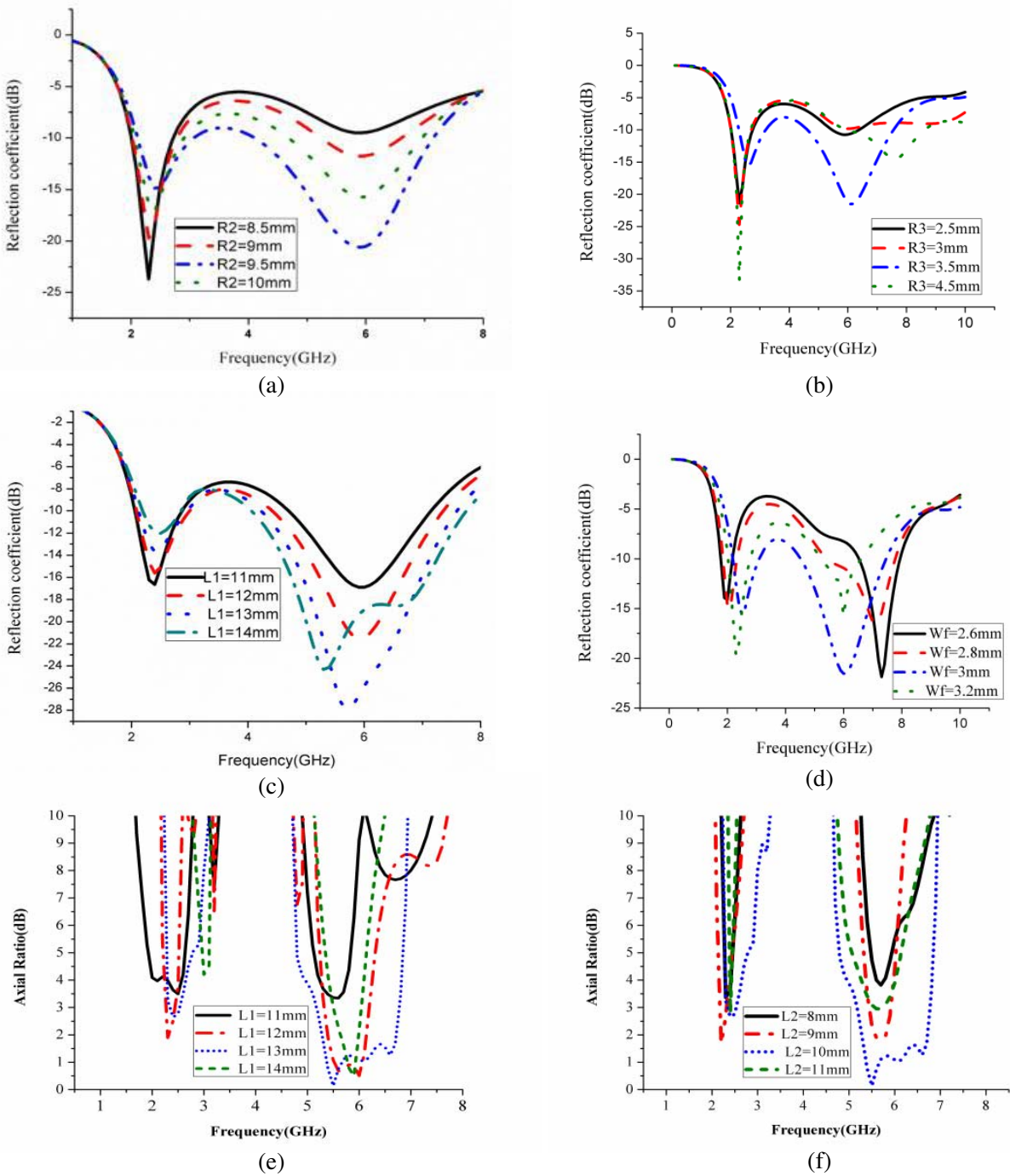


**Figure 3.** Parametric analysis of (a) varying the second circle radius. (b) Varying the third circle radius. (c) Length of ground. (d) Width of the feed. (e) Axial ratio variation for length of the ground ( $L_1$ ). (f) Axial ratio variation for length of the ground ( $L_2$ ).

varying parameters  $L_1$  and  $L_2$ . Figs. 6(e) and (f) show the parametric analyses of  $L_1$  and  $L_2$ , respectively. Parameter  $L_1$  is varied from 11 mm to 14 mm, and the observed maximum 3 dB axial ratio bandwidth is observed at  $L_1 = 13$  mm. Similarly, the length of the second ground ( $L_2$ ) is varied from 8 mm to 11 mm by fixing the  $L_1$  value to 13 mm, and the maximum 3 dB axial ratio bandwidth is observed at  $L_2 = 10$  mm. In Fig. 3(d), width of the feed ( $W_f$ ) is varied from 2.6 to 3.2 mm, and for feed

width 2.6 mm the fundamental resonant frequency shifted to 2 GHz and second resonant frequency to 7.7 GHz. For the selected value of  $W_f = 3$  mm, antenna resonates at required frequencies of 2.45 GHz and 5.8 GHz.

The surface current distribution of the proposed antenna is presented at two different frequencies of 2.45 GHz and 5.8 GHz in Fig. 4. The representation of current distribution is given at different time instants of  $0^\circ$ ,  $90^\circ$ ,  $180^\circ$  and  $270^\circ$ , respectively. At 2.45 GHz, the orientation of current elements is in anticlock wise direction which leads to right-hand circular polarisation (RHCP). Similarly at 5.8 GHz, the same kind of current distribution is observed. Fig. 5 represents the antenna reflection coefficient and axial ratio at different bending angles. The antenna performance is evaluated by bending antenna to  $30^\circ$ ,  $60^\circ$  and  $90^\circ$ . In the simulation study, as the bending angle increases, the reflection coefficient value at the second band of 5.8 GHz reaches minimum value, but at the lower frequency band of 2.45 GHz there is not much variation.

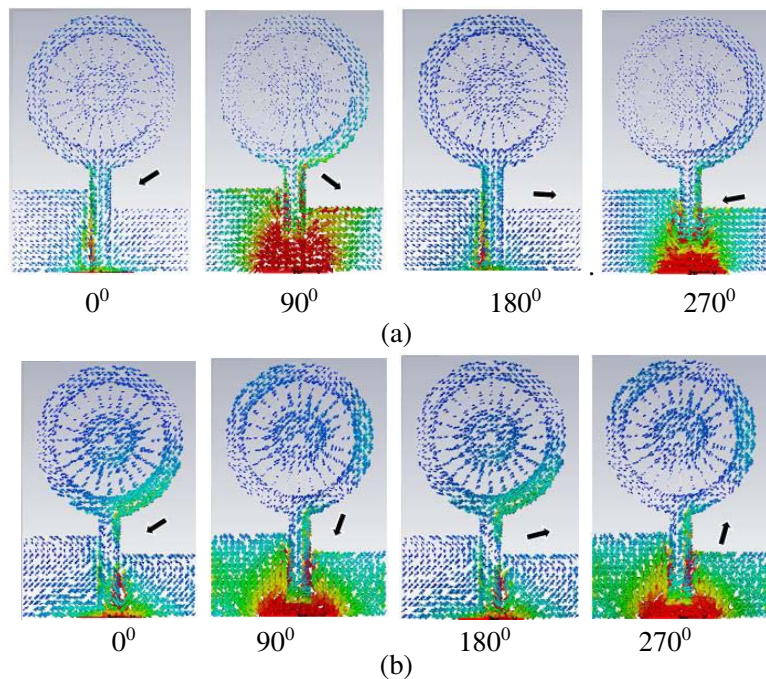


Figure 4. Surface current distribution at (a) 2.45 GHz, (b) 5.8 GHz.

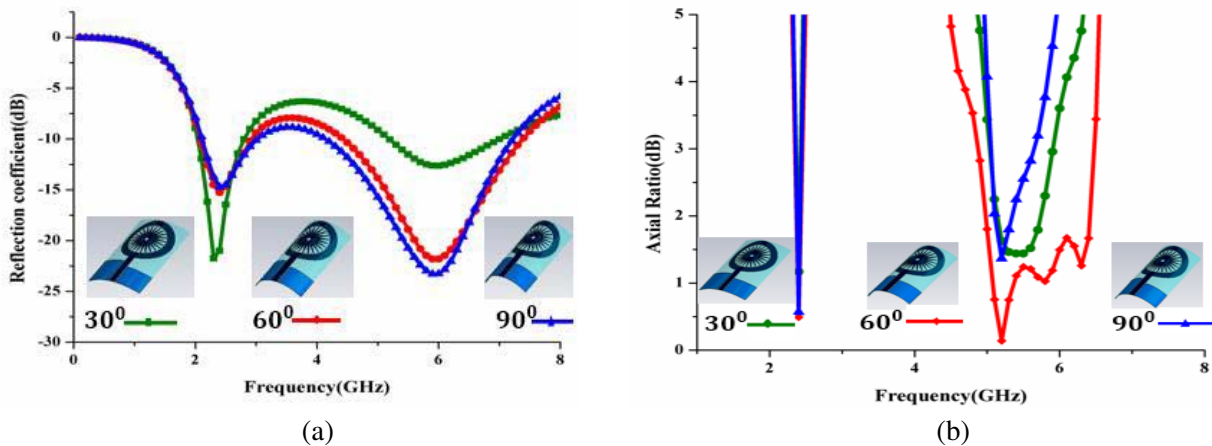
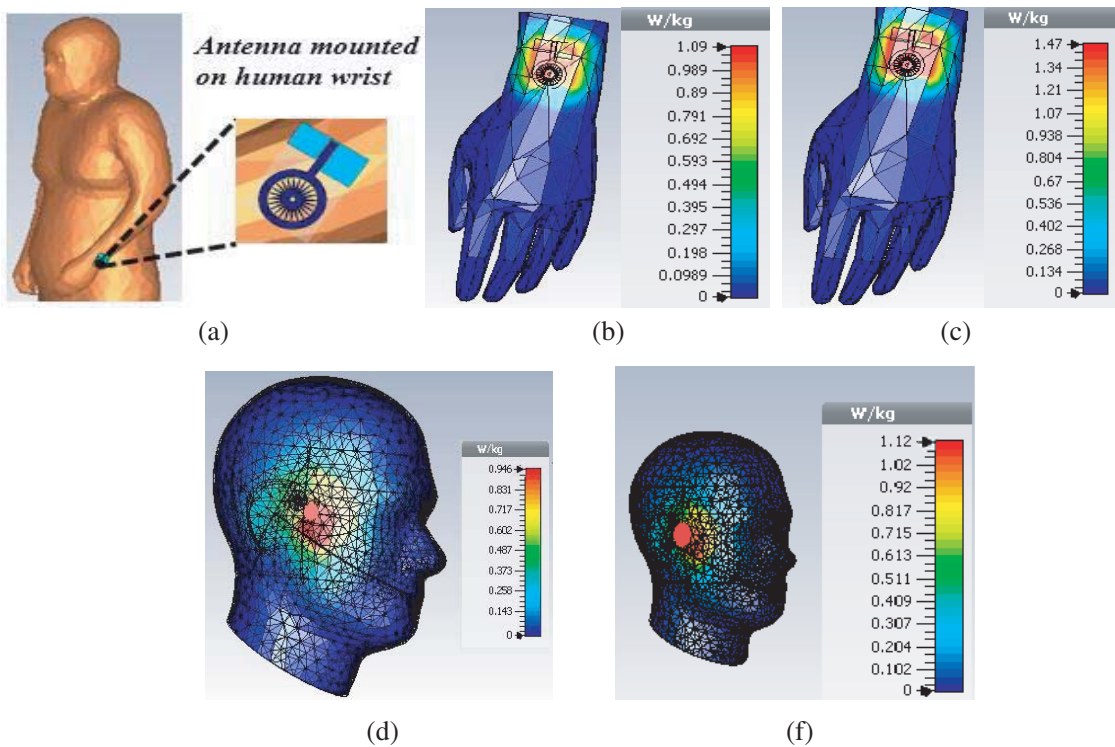


Figure 5. Proposed antenna. (a) Reflection coefficient. (b) Axial ratio.

#### 4. ON-BODY PLACEMENT ANALYSIS

As the antenna is designed for wearable applications it should be placed on the human body, and its functionality is analyzed. For doing the on-body analysis, the antenna is placed on the human body like CAD homogeneous model available in CST is taken. Generally, human body consists of high dielectric constant layers like skin, fat, muscle and bone which will influence the antenna performance.

In this case, voxel structure is too large, compared to antenna size which is shown in Fig. 6. To do SAR analysis, a three-dimensional anatomical hand and head phantom model is taken. The simulation of SAR is performed using finite-difference time domain (FDTD) method of computer simulation technology microwave studio (CST) [14–16]. The SAR values are evaluated on 1 gm biological tissue. An input power of 0.5 W was used in the simulation setup. The obtained SAR values of 1.09 w/kg and 0.946 W/Kg at 2.45 GHz and 1.47 w/kg and 1.12 W/Kg at 5.8 GHz can be observed on hand and head from Fig. 6. The observed values satisfy FCC and ICNIRP standards for which the values should be less than 1.6 w/kg averaged over 1 gm of tissue and 2 w/kg averaged over 10 gm of tissue.



**Figure 6.** (a) Antenna mounted on wrist and head (b), (d) SAR value at 2.45 GHz (c), (f) SAR value at 5.8 GHz.

The radiation field analysis is performed in Ansys savant simulation tool, which is based on shooting and bouncing rays method. The field distributions are calculated at resonating frequencies like 2.45 GHz and 5.8 GHz, and the far-field radiation patterns are presented using ANSYS Savant simulation tool in  $XZ$ ,  $YZ$ ,  $XY$ -planes as shown in Fig. 7. In  $XZ$ -plane and  $YZ$ -plane, the radiation patterns are dumbbell-shaped in free standing antenna at 2.45 GHz and 5.8 GHz. There is a slight variation of patterns when antenna is placed on human body. In the elevation planes at 2.45 GHz maximum distribution is observed at  $60^\circ$ – $70^\circ$  in  $YZ$ -plane. In the azimuth plane, radiation patterns are nearly omnidirectional in nature at two frequencies. At 5.8 GHz, the maximum radiation patterns are nearly directional in which maximum distribution is observed along  $60^\circ$  in  $XZ$ -plane and  $45^\circ$  in  $YZ$ -plane.

Fig. 8 presents simulated and measured reflection coefficients of the antenna. At the first resonating frequency, the simulation results are exactly matched with measured results, and for the second resonating frequency band, there is a slight mismatch between simulated and measured values. However,

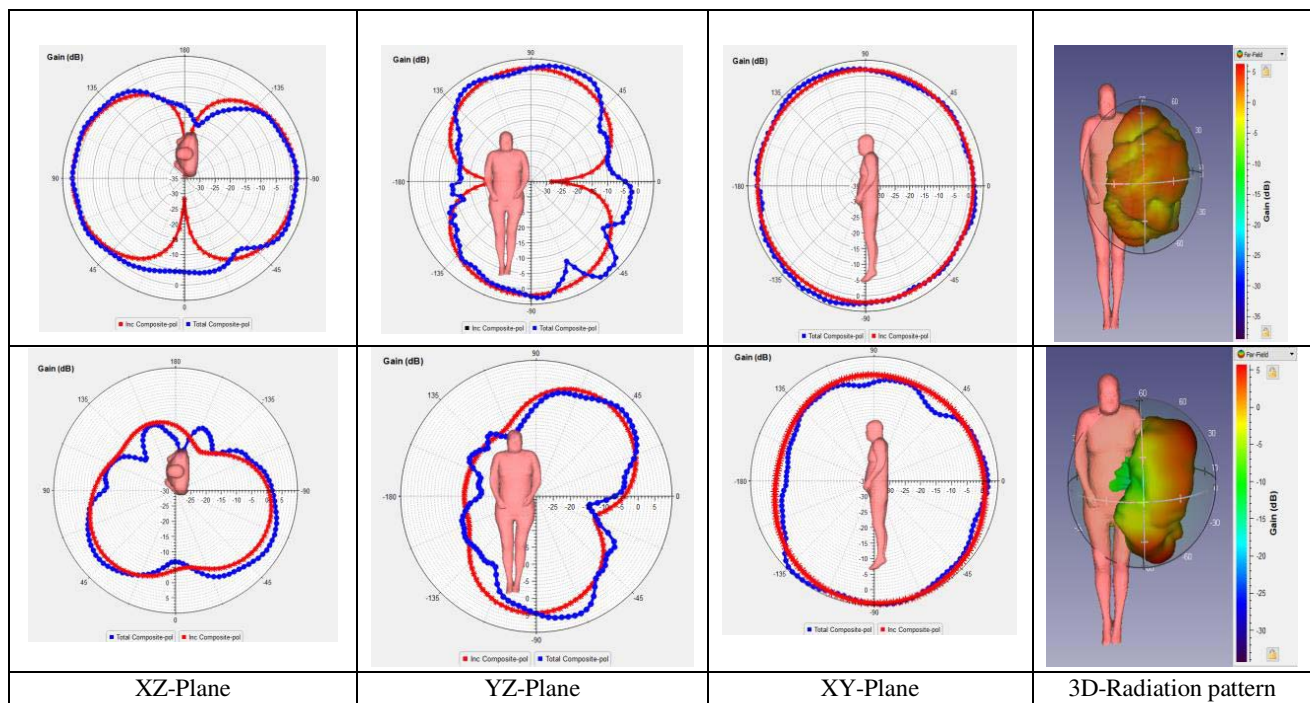
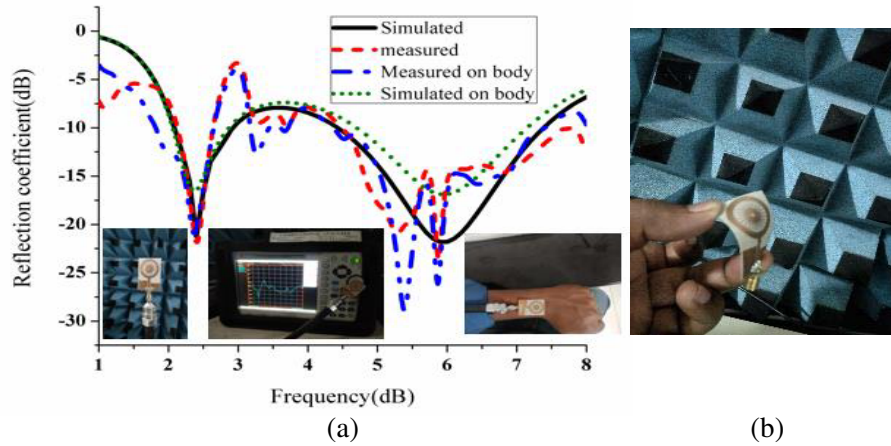


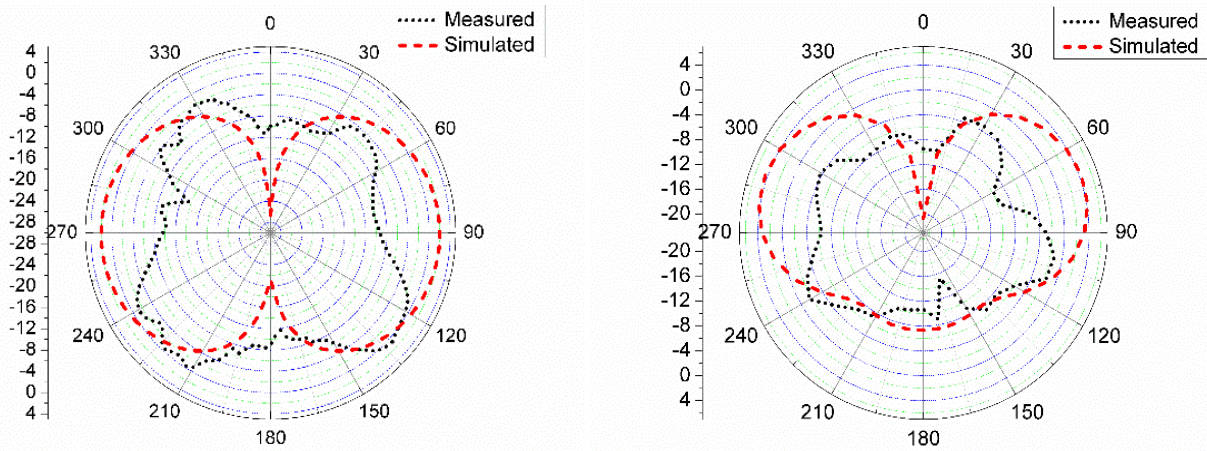
Figure 7. Simulated far field patterns of proposed antenna at 2.45 GHz and 5.8 GHz.

Table 2. Comparison of proposed antenna with previous works.

Ref	Size	Frequency Range (GHz)	Impedance bandwidth (%)	Peak Gain (dBi)	SAR Values (W/Kg)	Applications
[2]	$90 \times 124 \times 1$	1.78–1.98 2.38–2.505	10.92 5.08	-30.5 -22.2	5.77 6.62	GSM ISM
[4]	$30 \times 45 \times 3.2$	2.4–2.485 5.725–5.875	3.4 2.5	2.6 3.6	- -	ISM BANDS
[5]	$27 \times 28 \times 0.6$	0.38–0.47 2.27–2.57	12.4 16.1	3.09 0.64	5.42 4.70	MICS and ISM
[6]	$40 \times 40 \times 4.2$	0.4–0.405 2.35–2.57	1.2 8.9	0.49 2.3	0.05 1.13	MICS and ISM
[14]	$70 \times 70 \times 1.6$	1.54–1.62 2.67–2.87 3.33–3.46 5.24–5.42	5 7.2 3.8 3.7	1.41 3.56 1.8 2.38	0.2 0.607 0.603 0.347	GPS, WiMax and WiFi
[15]	$60 \times 23 \times 1.6$	1.75–2.25 2.3–2.6	25 12	- -	0.6 1.33	PCS/IMT- 2000/WLAN
[16]	$30 \times 50 \times 1.5$	2.16–2.75 7.14–9.91	23 33	2.275 3.151	1.514 1.82	WLAN and RFID
Proposed antenna	$40 \times 28 \times 0.4$	2.1–3.1 4.4–7.7	38 54	2.2 4.6	1.09 1.47	ISM/WLAN



**Figure 8.** Performance characteristics of the antenna. (a) Reflection coefficient, (b) flexible nature.



**Figure 9.** Simulated and measured  $E$ -plane radiation patterns at 2.45 GHz and 5.8 GHz.

the bandwidth coverages of both frequency bands for simulation and measurement are quite similar. The measured radiation patterns are compared with simulated ones in Fig. 9.

Table 2 is presented here for the comparison of the current antenna performance characteristics with previous literature. Compared with previous works, a significant improvement in gain and reduction in size can be observed. The SAR values also satisfy the FCC standards.

## 5. CONCLUSION

A dual-band antenna operating for ISM band and WLAN applications is designed in this work. The antenna is a novel circular ring-shaped antenna with 24 spokes and semi-flexible nature, which is more suitable for wearable applications. To analyse the performance in real time environment, the antenna is placed virtually on human body and validates the performance characteristics. The designed antenna providing a peak gain of 2.2 dBic at 2.45 GHz and 4.6 dBic at 5.8 GHz and providing dipole like radiation and omnidirectional radiation in  $E$  and  $H$ -planes, respectively. The observed SAR values of 1.09 W/Kg and 1.47 W/Kg on hand and 0.946 W/Kg and 1.12 W/Kg at 2.45 GHz and 5.8 GHz, respectively satisfy the FCC standards. Measured results of the proposed antenna correlate with simulation ones, and the current model can be implemented in wearable devices for the specified application bands to establish good communication link.

## REFERENCES

1. Zhu, D., Y.-X. Guo, M. Je, and D.-L. Kwong, "Design and in vitro test of a differentially fed dual-band implantable antenna operating at MICS and ISM bands," *IEEE Transactions on Antennas and Propagation*, Vol. 62, No. 5, 2430–2439, 2014.
2. Velan, S. and E. F. Sundarsingh, "Dual-band EBG integrated monopole antenna deploying fractal geometry for wearable applications," *IEEE Antennas and Wireless Propagation Letters*, Vol. 14, 249–252, 2015.
3. Tak, J., S. Woo, J. Kwon, and J. Choi, "Dual-band dual-mode patch antenna for on-/off-body WBAN communications," *IEEE Antennas and Wireless Propagation Letters*, Vol. 15, 348–351, 2016.
4. Deepak, U., T. K. Roshna, C. M. Nijas, K. Vasudevan, and P. Mohanan, "A dual band SIR coupled dipole antenna for 2.4/5.2/5.8 GHz applications," *IEEE Transactions on Antennas and Propagation*, Vol. 63, No. 4, 1514–1520, 2015.
5. Xu, L.-J., Z. Duan, and Y.-M. Tang, "A dual-band on-body repeater antenna for body sensor network," *IEEE Antennas and Wireless Propagation Letters*, Vol. 15, 1649–1652, 2016.
6. Kang, D.-G., J. Tak, and J. Choi, "Dual-band on-body antenna for in-on-on WBAN repeater applications," *Microwave and Optical Technology Letters*, Vol. 58, No. 2, 436–441, 2016.
7. Lu, L. and J. C. Coetzee, "A modified dual-band microstrip monopole antenna," *Microwave and Optical Technology Letters*, Vol. 48, No. 7, 1401–1403, 2006.
8. Yeung, S. H., K. F. Man, and W. S. Chan, "Optimised design of an ISM band antenna using a jumping genes methodology," *IET Microwaves, Antennas & Propagation*, Vol. 2, No. 3, 259–267, 2008.
9. Tak, J., D.-G. Kang, and J. Choi, "A compact dual-band monopolar patch antenna using  $TM_{01}$  and  $TM_{41}$  modes," *Microwave and Optical Technology Letters*, Vol. 58, No. 7, 1699–1703, 2016.
10. Zhu, X.-Q., Y.-X. Guo, and W. Wu, "A novel dual-band antenna for wireless communication applications," *IEEE Antennas and Wireless Propagation Letters*, Vol. 15, 516–519, 2016.
11. Tran, H. H. and I. Park, "Wideband circularly polarized cavity-backed asymmetric crossed bowtie dipole antenna," *IEEE Antennas and Wireless Propagation Letters*, Vol. 15, 358–361, 2016.
12. Tu, T. L., H. H. Tran, and H. C. Park, "A simple penta-band circularly polarized cpw-fed monopole-patch antenna covering six commercial application bands," *Microwave and Optical Technology Letters*, Vol. 60, No. 3, 773–778, 2018.
13. Zahran, S. R., M. A. Abdalla, and A. Gaafar, "Time domain analysis for foldable thin UWB monopole antenna," *AEU-International Journal of Electronics and Communications*, Vol. 83, 253–262, 2018.
14. Saygin, H., V. Rafiei, and S. Karamzadeh, "A new compact dual band CP antenna design," *Microwave and Optical Technology Letters*, Vol. 60, No. 3, 594–600, 2018.
15. Sajal, S., B. D. Braaten, T. Tolstedt, S. Asif, and M. J. Schroeder, "Design of a conformal monopole antenna on a paper substrate using the properties of graphene-based conductors," *Microwave and Optical Technology Letters*, Vol. 59, No. 6, 1279–1283, 2017.
16. Ahmed, M. I., M. F. Ahmed, and A. E. H. Shaalan, "SAR calculations of novel wearable fractal antenna on metamaterial cell for search and rescue applications," *Progress In Electromagnetics Research*, Vol. 53, 99–110, 2017.
17. Shin, C. S., D. G. Choi, N. Kim, and J. I. Choi, "Internal monopole antenna design for multi-band operation and SAR analysis," *PIERS Proceedings*, 294–297, Hangzhou, Zhejiang, China, Aug. 22–26, 2005.
18. Ahmed, M. I., E. A. Abdallah, and H. M. Elhennawy, "Novel wearable eagle shape microstrip antenna array with mutual coupling reduction," *Progress In Electromagnetics Research B*, Vol. 62, 87–103, 2015.